

Original paper

Pokhodyashinite, $\text{CuTlSb}_2(\text{Sb}_{1-x}\text{Tl}_x)\text{AsS}_{7-x}$, a new thallium sulfosalts from the Vorontsovskoe gold deposit, Northern Urals, Russia

Anatoly V. KASATKIN^{1*}, Jakub PLÁŠIL², Emil MAKOVICKÝ³, Radek ŠKODA⁴,
Atali A. AGAKHANOV¹, Mikhail V. TSYGANKO⁵

¹ Fersman Mineralogical Museum of Russian Academy of Sciences, Leninsky Prospekt 18–2, 119071 Moscow, Russia; anatoly.kasatkin@gmail.com

² Institute of Physics, Academy of Sciences of the Czech Republic v.v.i, Na Slovance 1999/2, Prague 8, 182 21, Czech Republic

³ Department of Geoscience and Resource Management, University of Copenhagen, Østervoldgade 10, DK–1350, Copenhagen K, Denmark

⁴ Department of Geological Sciences, Faculty of Science, Masaryk University, Kotlářská 2, 611 37, Brno, Czech Republic

⁵ ul. 40 let Oktyabrya 15, Kalya, Severouralsk, Sverdlovskaya Oblast', 624474 Russia

* Corresponding author



Pokhodyashinite $\text{CuTlSb}_2(\text{Sb}_{1-x}\text{Tl}_x)\text{AsS}_{7-x}$, is a new sulfosalts from the Vorontsovskoe gold deposit, Sverdlovsk Oblast', Northern Urals, Russia. It forms anhedral grains up to 0.1×0.05 mm in size in calcite and is associated with major orpiment, pyrite, realgar and minor baryte, clinocllore, As-bearing fluorapatite, harmotome, prehnite, native gold and a rich spectrum of sulfosalts. Pokhodyashinite is black, opaque, and has a metallic luster and a black streak. It is brittle, with an uneven fracture and poor cleavage on {100}. The Vickers hardness (VHN, 20 g load) is 55 kg/mm², corresponding to a Mohs hardness of 2. The calculated density is 5.169 g/cm³. In reflected light, pokhodyashinite is grayish-white, bireflectance is distinct. In crossed polars, it is strongly anisotropic; rotation tints vary from dark brownish gray to light bluish-gray. No internal reflections are observed. The reflectance values for wavelengths recommended by the Commission on Ore Mineralogy of the IMA are (R_{\min}/R_{\max} , %): 28.9/34.6 (470 nm), 27.6/33.4 (546 nm), 26.7/32.4 (589 nm), 26.1/31.1 (650 nm). The empirical formula of pokhodyashinite based on $\Sigma\text{Me} = 6 \text{ apfu}$ is $\text{Cu}_{0.700}\text{Ag}_{0.340}\text{Tl}_{1.320}\text{Pb}_{0.020}\text{Sb}_{2.630}\text{As}_{0.990}\text{S}_{6.625}$. Pokhodyashinite is monoclinic, space group $C2/m$, $a = 23.431(5)$, $b = 3.996(2)$, $c = 14.070(3)$ Å, $\beta = 110.23(3)^\circ$, $V = 1236.1(8)$ Å³ and $Z = 4$. Its structure can be described as wavy slabs of a complex structure based on double-rods of Sb-coordination pyramids and lone-electron-pair interspaces/micelles, separated by wavy interlayers consisting of paired columns of Tl and rods of paired Cu-coordination polyhedra. A small amount of Tl-for-Sb substitution results in partial anion vacancies in one sulfur site. The new mineral is named in honor of Maxim Mikhailovitch Pokhodyashin, a pioneer of mining engineering and smelting works in the Northern Urals of the 18th century.

Keywords: pokhodyashinite, new mineral, copper, thallium, sulfosalts, crystal structure, Vorontsovskoe gold deposit, Northern Urals

Received: 15 February 2022; **accepted:** 6 April 2022; **handling editor:** J. Sejkora

The online version of this article (doi: 10.3190/jgeosci.342) contains supplementary electronic material.

1. Introduction

Over the last few years, the Vorontsovskoe gold deposit at Northern Urals (Russia) became known worldwide due to its unique Tl–Hg–Mn–As–Sb–S mineralization. Our team has systematically studied its mineralogy since 2013. We defined nine major ore mineral assemblages, including seven related to carbonate breccias, and described 210 mineral species reliably identified at the deposit (Kasatkin et al. 2022b). By this number, the Vorontsovskoe deposit is noticeably ahead of three other deposits famous for their Tl–Hg–As–Sb-mineralization: Lengenbach in Switzerland (160 species – see Raber and Roth 2018), Allchar in North Macedonia (85 species – see Boev et al. 2012; www.mindat.org) and Jas Roux in France (53 species – see Bourgoin et al. 2011; www.mindat.org). The largest and most interesting group of minerals

discovered at the Vorontsovskoe deposit unambiguously consists of sulfosalts. Seventy-five minerals of this group were identified at the deposit, including nine new mineral species: clerite (Murzin et al. 1996), vorontsovite, ferrovorontsovite (Kasatkin et al. 2018b), tsygankoite (Kasatkin et al. 2018a), gladkovskyite (Kasatkin et al., 2019), luboržákite (Kasatkin et al. 2020a), auerbakhite (Kasatkin et al. 2021a), gungerite (Kasatkin et al. 2022a) and pokhodyashinite described herein.

Pokhodyashinite (pronouncing: po kho dya shi nait; Russian Cyrillic походяшинит) is named in honor of Maxim Mikhailovitch Pokhodyashin (Максим Михайлович Походяшин, 1708–1780), Russian merchant born at Verkhotur'e (now – the city in Sverdlovskaya Oblast'), manufacturer, owner of mines and smelter plants in Northern Urals. He was a pioneer of mining engineering and smelting works in the region, founded

the Bogoslovskiy mining district, opened and operated the now-famous Turyinsk copper Mines (Fig. 1), established three copper smelters including Petropavlovskiy and Bogoslovskiy plants which yielded up to 90 % of Urals' copper in Russia in the second half of the 18th century and built important roads connecting the mines with the smelters. In the 1770s, he prospected the gold in the area but without success. Settlements founded during the building and exploitation of his mines and plants later became the largest cities of Northern Urals: Krasnoturyinsk, Severouralsk and Karpinsk. Thanks to M.M. Pokhodyashin, this hitherto almost uninhabited part of Urals started to grow and develop.

The new mineral and its name have been approved by the Commission on New Minerals, Nomenclature and Classification (CNMNC) of the International Mineralogi-

cal Association (IMA 2019–130). The holotype specimen is deposited in the collections of the Fersman Mineralogical Museum of the Russian Academy of Sciences, Moscow, Russia, with the registration number 5517/1.

First short data on pokhodyashinite published in the Newsletter of the CNMNC (Kasatkin et al. 2020b) and by Kasatkin et al. (2021b) reported on it as a triclinic mineral with space group $P-1$ and ideal formula $Cu_2Tl_3Sb_5As_2S_{13}$. However, since some ambiguities in the interpretation of structural data remained, and due to the absence of new material of better quality, we have decided to restudy the crystal from the original structure determination using new measurement conditions (see below). The obtained new data turned up of substantially higher completeness and better quality and showed that the lattice of pokhodyashinite displays monoclinic symmetry instead of triclinic. They also resulted in a slight change of the ideal formula where, remarkably, Ag was added as an important element in the stabilization of the structure and the structural nature of the observed anion deficiency was resolved.

2. Occurrence

A detailed description of the Vorontsovskoe gold deposit, its genesis, geology, the composition of main types of ores and features of ore-bearing breccias are found elsewhere (Sazonov et al. 1998; Vikentyev et al. 2016; Murzin et al. 2017; Stepanov et al. 2017, 2021; Kasatkin et al., 2019, 2020a, 2021a). The most recent summary of the history of the study of the deposit, its geological background, a detailed description of main mineral assemblages and all mineral species reliably identified to date were given by Kasatkin et al. (2022b).

Fig. 1 Memorial complex “Copper Mountain” dedicated to the founder of Krasnotur’insk town Maksim Mikhailovitch Pokhodyashin. The complex is located in the center of the town, exactly in the place where Pokhodyashin built Vasilievskiy copper mine in 1760 – the first of the famous Tur’insk copper Mines. Photo: A. V. Kasatkin, august 2018.





Fig. 2 Main ore stockpile of the Vorontsovskoe deposit where specimens containing pokhodyashinite were collected. Photo: A. V. Kasatkin, august 2018.

Pokhodyashinite, so far, is the rarest of the new mineral species discovered at the Vorontsovskoe deposit. It has been found in two polished sections only, made from a fragment of carbonate breccia collected in October 2017 by one of the authors (M.V.T.) at the main ore stockpile of the deposit located near the Northern open-pit (Fig. 2). GPS coordinates of the sampling area are $59^{\circ}38'51.4''$ N and $60^{\circ}12'52.7''$ E. Pokhodyashinite occurs in mineral assemblage No. 1, also known as a boscardinite–écrintsite assemblage (Kasatkin et al. 2022b). The latter encloses the highest number of ore minerals, including very rare thallium sulfosalts. Pokhodyashinite was identified in carbonate breccia composed mainly of calcite and cemented by major orpiment, pyrite, realgar, and minor baryte, clinocllore, fluorapatite (As-bearing), harmotome and prehnite. Other minerals directly associated with pokhodyashinite include arsiccioite, boscardinite, chabournéite, coloradoite, dalnegroite, écrintsite, gold, parapierronite, routhierite, sicherite, sphalerite, stalderite, tennantite-(Zn) and weissbergite. The above paragenesis results from the interaction between post-magmatic hydrothermal solutions and carbonate rocks.

3. Physical and optical properties

Pokhodyashinite forms scarce anhedral grains up to 0.1×0.05 mm in size embedded in the calcite matrix (Fig. 3). Pokhodyashinite is black, opaque, and has a metallic luster and a black streak. It is brittle, with an uneven fracture and poor cleavage, probably on $\{100\}$. The Vickers hardness (VHN, 20 g load) is 55 kg/mm^2 (range

$50\text{--}61$, $n = 3$), corresponding to a Mohs hardness of 2. Its density could not be measured because of the absence of corresponding heavy liquids and the paucity of available material. The density calculated from the empirical formula ($Z = 4$) and the unit-cell volume determined from the single-crystal X-ray diffraction data is 5.169 g/cm^3 . In reflected light, pokhodyashinite is grayish-white; bireflectance is distinct. Under crossed polars, it is strongly anisotropic; rotation tints vary from dark brownish gray to light bluish-gray. No internal reflections are observed. The reflectance values for wavelengths recommended by the Commission on Ore Mineralogy of the IMA are (R_{\min}/R_{\max} , %): 28.9/34.6 (470 nm), 27.6/33.4 (546 nm),

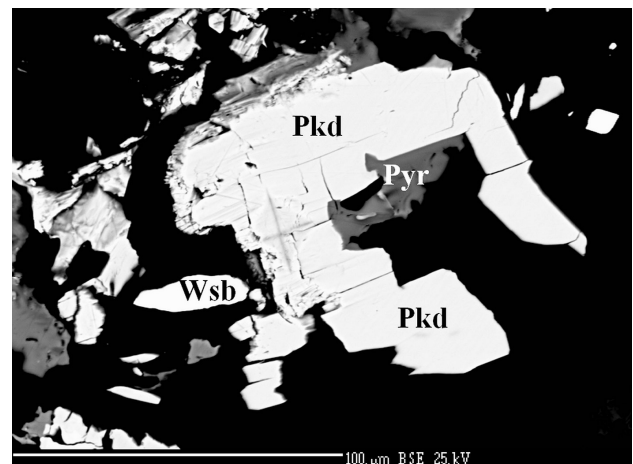


Fig. 3 Anhedral grain of pokhodyashinite (Pkd) in calcite matrix (black) with weissbergite (Wsb) and pyrite (Pyr). This grain is the largest found and its fragment was extracted after EMPA and used for structural studies. Polished section. SEM (BSE) image.

Tab. 1 Reflectance values of pokhodyashinite (measured in air)

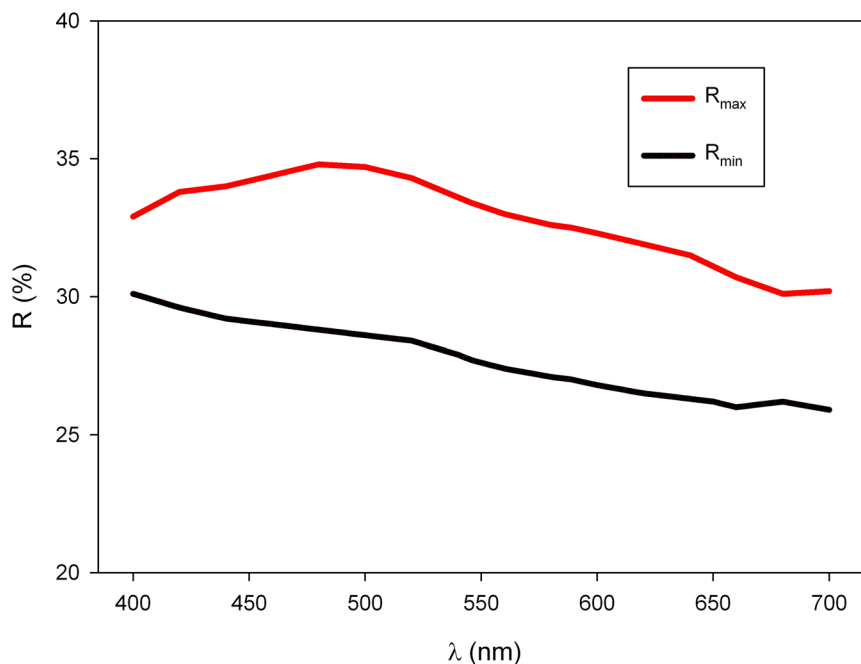
R_{\max}	R_{\min}	λ (nm)	R_{\max}	R_{\min}	λ (nm)
32.9	30.1	400	33.0	27.4	560
33.8	29.6	420	32.6	27.1	580
34.0	29.2	440	32.4	26.7	589 (COM)
34.4	29.0	460	32.3	26.8	600
34.6	28.9	470 (COM)	31.9	26.5	620
34.8	28.8	480	31.5	26.3	640
34.7	28.6	500	31.1	26.1	650 (COM)
34.3	28.4	520	30.7	26.0	660
33.6	27.9	540	30.1	26.2	680
33.4	27.6	546 (COM)	30.2	25.9	700

27.0/32.5 (589 nm), 26.2/31.1 (650 nm). The full set of reflectance measurements performed in the air relative to a WTiC standard employing a Universal Microspectrophotometer UMSP 50 (Opton-Zeiss, Germany) is given in Tab. 1 and plotted in Fig. 4.

4. Chemical composition

Preliminary semi-quantitative chemical analyses using a scanning electron microscope CamScan 4D (Fersman museum, Moscow) equipped with INCA Energy micro-analyzer (EDS mode, 20 kV, 5 nA and beam diameter 5 μm) showed the presence of essential Cu, Ag, Tl, As, Sb, S, and minor Pb in pokhodyashinite. However, contents of other elements with atomic numbers higher than that of carbon were below detection limits.

Quantitative chemical analyses were conducted in the wavelength-dispersive (WDS) mode, using a Cameca SX-100 electron microprobe (Masaryk University, Brno)

**Fig. 4** Reflectivity curves for pokhodyashinite in air.**Tab. 2** Chemical data (in wt. %) for pokhodyashinite

Constituent	Mean	Range	Stand. Dev.	Reference material
Cu	4.59	4.47–4.71	0.10	Cu
Ag	3.79	3.62–3.86	0.09	Ag
Tl	27.88	27.36–28.15	0.28	Tl(Br,I)
Pb	0.42	0.38–0.52	0.05	PbSe
As	7.63	7.40–7.83	0.15	pararammelsbergite
Sb	32.95	32.62–33.73	0.41	Sb
S	21.89	21.55–22.49	0.45	chalcopyrite
Total	99.15			

operated at 25 kV and 20 nA with a beam size of 1 μm . Peak counting times were 20 s for all elements, with one-half of the peak time for each background. The following standards, X-ray lines, and crystals (in parentheses) were used: Cu: Cu metal, K_{α} (LLIF); Ag: Ag metal, L_{α} (PET); Tl: Tl(Br,I), M_{α} (PET); Pb: PbSe, M_{α} (LPET); As: pararammelsbergite, L_{β} (TAP); Sb: Sb, L_{β} (PET); S: chalcopyrite, K_{α} (LPET). Raw X-ray intensities were corrected for matrix effects with a $\phi(\rho z)$ algorithm of X-PHI routine (Merlet 1994).

Analytical data are given in Tab. 2 (mean of 6 analyses). No other elements with atomic numbers higher than 8 were detected.

The empirical formula on the basis of $\Sigma Me = 6 \text{ apfu}$ is $\text{Cu}_{0.700}\text{Ag}_{0.340}\text{Tl}_{1.320}\text{Pb}_{0.020}\text{Sb}_{2.630}\text{As}_{0.990}\text{S}_{6.625}$ ($Z = 4$). The error on the electrostatic balance is good, with $E_v(\%) = +0.10$. Probably, minor Pb occurs in pokhodyashinite according to the substitution rule $2\text{Pb}^{2+} = \text{Tl}^{+} + \text{Sb}^{3+}$. Thus, the chemical formula, corrected for minor Pb, is $\text{Cu}_{0.70}\text{Ag}_{0.34}\text{Tl}_{1.33}\text{Sb}_{2.64}\text{As}_{0.99}\text{S}_{6.625}$ ($Z = 4$). If significant, the slight Ag excess with respect to $(\text{Cu} + \text{Ag}) = 1 \text{ apfu}$ may replace Sb^{3+} , along with major Tl. The crystal-

chemical formula, taking into account the structural model, could be written as $\text{Cu}^1(\text{Cu}_{0.70}\text{Ag}_{0.30})^{\text{Tl}1}\text{Tl}_{1.00}\text{Sb}^1\text{Sb}_{1.00}^{\text{Sb}2}(\text{Sb}_{0.63}\text{Tl}_{0.33}\text{Ag}_{0.04})^{\text{Sb}3}\text{Sb}_{1.00}^{\text{As}4}(\text{As}_{0.99}\text{Sb}_{0.01})\text{S}_{6.63}^*$.

The substitution of Sb^{3+} by Tl^{+} is not unusual. It occurs, e.g., in the Pb-free chabournéite (Makovicky et al. 2021). Its consequences will be described in the structural part of the paper. This substitution explains the observed S content, i.e., 6.625 apfu, to be compared with a theoretical agreement with an 'excess' of $(\text{Tl} + \text{Ag}) = 0.37 \text{ apfu}$. The formula of pokhodyashinite can be written as $\text{CuTlSb}_2(\text{Sb}_{1-x}\text{Tl}_x)\text{AsS}_{7-x}$, a rare case of anion vacancies among sulfosalts.

This formula is in agreement with the formula obtained from the crystal structure refinement, $\text{Ag}_{0.313}\text{Tl}_{1.226}\text{Sb}_{2.774}\text{AsCu}_{0.687}\text{S}_{6.532}$ with $R_1 = 7.58\%$.

5. X-ray crystallography

A blocky fragment of pokhodyashinite, $45 \times 35 \times 13 \mu\text{m}$ in size, extracted from the polished section used for EPMA investigations (Fig. 3), the same one as used for the structure study for the approval process by the CNMNC, was restudied with a Rigaku SuperNova single-crystal diffractometer equipped with an Atlas S2 CCD detector and a microfocus MoK_α source. The new data collection comprised an increased counting time per frame (of 1200 seconds per 1°) compared to the previous dataset (500 seconds per 1°) and provided more unique observed reflections, 975 vs. 775 with $I > 3\sigma(I)$. The new data of the much higher completeness showed that the reciprocal lattice of pokhodyashinite indicates a monoclinic structure (instead of triclinic), space group $C2/m$, $a = 23.431(5)$, $b = 3.996(2)$, $c = 14.070(3) \text{ \AA}$, $\beta = 110.23(3)^\circ$, $V = 1236.1(8) \text{ \AA}^3$ and $Z = 4$. Data reduction was performed using CrysAlisPro Version 1.171.39.35c (Rigaku 2019). The data were corrected for Lorentz factor, polarization effect and absorption (multi-scan, ABSPACK scaling algorithm; Rigaku 2019). The crystal structure of pokhodyashinite was solved from the X-ray data using the intrinsic phasing algorithm of the SHELXT program (Sheldrick 2015) and refined by the software Jana2020 (Petříček et al. 2020). The crystal data and the experimental details are given in Tab. 3, atom coordinates, atomic displacement parameters and site occupancies in Tab. 4, anisotropic displacement parameters in Tab. 5 and selected interatomic distances in Tab. 6. The CIF file is deposited at the Journal's webpage www.jgeosci.org. Due to the lack of material for performing a conventional powder diffraction experiment,

Tab. 3 Summary of data collection conditions and refinement parameters for pokhodyashinite

Chemical formula sum	$\text{Ag}_{0.313}\text{Tl}_{1.226}\text{Sb}_{2.774}\text{AsCu}_{0.687}\text{S}_{6.532}$
Crystal system	monoclinic
Space group	$C2/m$ (#12)
Unit-cell parameters: a, b, c [Å]; β [$^\circ$]	23.341(5), 3.996(2), 14.070(3), 110.23(3)
Unit-cell volume [Å^3]	1236.1(8)
Z	4
Calculated density [g/cm^3]	5.105 (for the formula from the structure)
Crystal size [mm]	$0.045 \times 0.035 \times 0.013$
Diffractometer	Rigaku SuperNova with Atlas S2 CCD
Temperature [K]	291
Radiation, wavelength [Å]	MoK_α , 0.71073 (50 kV, 30 mA)
θ range for data collection [$^\circ$]	2.79–29.55
Limiting Miller indices	$h = -31 \rightarrow 32, k = -5 \rightarrow 5, l = -19 \rightarrow 19$
Axis, frame width ($^\circ$), time per frame (s)	ω , 1.0, 1200
Total reflections collected	14209
Unique reflections	1828
Unique observed reflections, criterion	975, [$I > 3\sigma(I)$]
Absorption coefficient [mm^{-1}], type	27.39; multi-scan
T_{\min}/T_{\max}	0.656/1.000
Data completeness to θ_{\max} (%), R_{int}	92, 0.120
Structure refinement	Full-matrix least-squares on F^2
No. of param., restraints, constraints	86, 0, 18
R, wR (obs)	0.0788, 0.1531
R, wR (all)	0.1536, 0.1705
GOF obs/all	2.25, 1.80
Weighting scheme, weights	$\sigma, w = 1/(\sigma^2(I) + 0.0004I^2)$
Largest diffraction peak and hole ($e^{-}/\text{Å}^3$)	2.92 (1.047 Å from Cu1/Ag1), –2.59

Tab. 4 Atom positions and equivalent displacement parameters (in Å^2) for pokhodyashinite

Atom	Occupancy	x/a	y/b	z/c	U_{eq}
Tl1		0.30974 (6)	0.5	0.83640(9)	0.0410(5)
Sb1		0.44839 (9)	1	0.73575(16)	0.0382(10)
Sb2/Tl2	0.785(15)/0.216(15)	0.56773(11)	0	0.60163(13)	0.0530(10)
Sb3/Tl3	0.988(14)/0.012(14)	0.32061(9)	0.5	0.5157(2)	0.0523(12)
Cu1/Ag1	0.69(3)/0.31(3)	0.55242(18)	0.5	0.9509(4)	0.089(2)
As1		0.65560(18)	0	0.8691(3)	0.083(2)
S1	0.97(2)	0.4301(3)	0.5	0.5676(5)	0.026(3)
S2		0.3355(3)	1	0.6691(5)	0.027(2)
S3		0.4483(3)	0.5	0.8564(5)	0.028(3)
S4	0.91(2)	0.6845(3)	0	0.6211(5)	0.027(3)
S5		0.6094(4)	0	0.9834(6)	0.045(3)
S6	0.65(3)	0.7168(5)	–0.5	0.9309(10)	0.087(9)
S7		0.5840(5)	0.5	0.7325(10)	0.171(11)

only the calculated powder pattern is given in Tab. 7. The theoretical d_{hkl} and relative intensities were calculated using the PowderCell program (Kraus and Nolze 1996).

In spite of the unambiguous results from the lattice of the mineral, results of the structure refinement show that the crystal is twinned, apparently on (010), and it is impossible to see whether it is monoclinic, without a reflection plane (010), or it is triclinic with the complete lattice overlap (merohedral twin). Traces of possible superstructure reflections indicating a very weakly

Tab. 5 Anisotropic displacement parameters (in Å²) for pokhodyashinite

	U^{11}	U^{22}	U^{33}	U^{12}	U^{13}	U^{23}
Tl1	0.0391(7)	0.0377(8)	0.0503(8)	0	0.0206(6)	0
Sb1	0.0357(12)	0.0220(12)	0.0673(15)	0	0.0308(11)	0
Sb2/Tl2	0.0905(19)	0.0270(13)	0.0362(12)	0	0.0149(11)	0
Sb3/Tl3	0.0233(12)	0.0267(14)	0.109(2)	0	0.0248(12)	0
Cu1/Ag1	0.045(3)	0.036(3)	0.147(5)	0	-0.018(3)	0
As1	0.054(2)	0.161(5)	0.0262(18)	0	0.0053(17)	0
S1	0.019(4)	0.029(5)	0.029(4)	0	0.006(3)	0
S2	0.033(4)	0.019(4)	0.031(4)	0	0.012(3)	0
S3	0.033(4)	0.028(4)	0.029(4)	0	0.018(3)	0
S4	0.029(5)	0.030(5)	0.020(4)	0	0.006(3)	0
S5	0.050(5)	0.053(6)	0.033(4)	0	0.014(4)	0
S6	0.013(7)	0.21(2)	0.035(8)	0	0.004(6)	0
S7	0.036(6)	0.37(3)	0.080(8)	0	-0.014(6)	0

Tab. 6 Selected interatomic distances (Å) in pokhodyashinite

Tl1–S2 ⁱ	3.298(7)	Sb1–S1	3.011(6)
Tl1–S2	3.298(7)	Sb1–S1 ⁱⁱ	3.011(6)
Tl1–S3	3.160(8)	Sb1–S2	2.482(7)
Tl1–S4 ^{iv}	3.412(6)	Sb1–S2 ⁱⁱ	2.704(5)
Tl1–S5 ⁱⁱⁱ	3.269(6)	Sb1–S3	2.623(5)
Tl1–S5 ^v	3.269(6)	Sb1–S3 ⁱⁱⁱ	2.623(5)
Tl1–S6 ^{iv}	3.537(12)	Sb1–S7	3.769(11)
Tl1–S6 ^{vi}	3.537(12)	Sb1–S7 ⁱⁱ	3.769(11)
Tl1–S6 ^v	3.536(15)		
		Sb3/Tl3–S1	2.412(7)
Sb2/Tl2–S1 ^{ix}	3.122(6)	Sb3/Tl3–S2 ⁱ	2.872(6)
Sb2/Tl2–S1 ^{viii}	3.122(6)	Sb3/Tl3–S2	2.872(6)
Sb2/Tl2–S4	2.654(8)	Sb3/Tl3–S4 ^{viii}	2.748(6)
Sb2/Tl2–S7 ⁱ	2.649(9)	Sb3/Tl3–S4 ^{vi}	2.748(6)
Sb2/Tl2–S7	2.649(9)		
		Cu1/Ag1–S3	2.340(8)
As1–S5	2.228(11)	Cu1/Ag1–S3 ⁱⁱⁱ	2.717(10)
As1–S6	2.438(7)	Cu1/Ag1–S5	2.358(5)
As1–S6 ⁱⁱ	2.438(7)	Cu1/Ag1–S5 ⁱⁱ	2.358(5)

Symmetry codes: (i) $x, y-1, z$; (ii) $x, y+1, z$; (iii) $-x+1, y, -z+2$; (iv) $x-1/2, y+1/2, z$; (v) $-x+1, y+1, -z+2$; (vi) $x-1/2, y+3/2, z$; (vii) $-x+1, y+1, -z+1$; (viii) $-x+1, y, -z+1$; (ix) $-x+1, y-1, -z+1$; (x) $-x+1/2, y-1/2, -z+1$; (xi) $-x+1/2, y+1/2, -z+1$; (xii) $-x+1, y-1, -z+2$; (xiii) $-x+3/2, y+1/2, -z+2$; (xiv) $-x+3/2, y-1/2, -z+2$

expressed superstructure along the [010] direction were observed but remain uncertain and too weak to integrate.

6. Description of the crystal structure and discussion

The structure of pokhodyashinite (Fig. 5) contains thirteen atomic sites: one site occupied by Tl, three mixed sites that either contain Sb, or mixed Sb and Tl, one site occupied by As, seven S sites, and one mixed-occupied Cu/Ag site.

Pokhodyashinite is one of the few structures which are rather complicated and do not belong strictly to one

homologous or plesiotype series, but show clear relations to several sulfosalt groups at the same time. The pokhodyashinite structure can be described as wavy slabs of a complex structure, which is based on double-layer rods of (primarily) Sb-coordination pyramids and lone-electron-pair (LEP) interspaces/micelles. They are separated by wavy interlayers consisting of paired columns of Tl, and from [010] rows of As, accompanied by rods of paired Cu-coordination polyhedra.

One aspect of pokhodyashinite structure is that the double-layer rods (narrow ribbons) of a chiefly Sb-based slab in it are similar (at least partly) to the rods in the structures of hutchinsonite $\text{TlPbAs}_5\text{S}_9$, jentschite $\text{TlPbAs}_2\text{SbS}_6$ and edenharterite $\text{TlPbAs}_3\text{S}_6$ (Takéuchi et al. 1965; Matsushita and Takéuchi 1994; Berlepsch 1996; Makovicky 2018; Berlepsch et al. 2000). One surface of such ribbons in these structures contains two coordination pyramids of LEP elements (primarily As) but the opposite surface consists of only one polyhedron, which is occupied by Pb in all three of them. This polyhedron is flanked on both sides by cation rows with alternation of Tl polyhedra and As pyramids.

The double-ribbon in pokhodyashinite is very similar; the differences are as follows: the central lone polyhedron is occupied by Sb (similar to As in imhofite) and not by M^{2+} , one side of the ribbon is flanked by Tl without intervening As, and the other side is flanked by As in a polyhedron which is rotated against those in the above minerals. Thus, the divalent (Tl+As) average of the flanking association from the above minerals is lost and other means of charge compensation are required.

The tightly-bonded ribbon in pokhodyashinite consists of the Sb1 and Sb2 pyramids on one surface and the Sb3 coordination pyramid on the opposite surface of the ribbon is flanked by a Tl polyhedron only from one side.

The Sb1 pyramid has the short Sb–S bond of 2.482 Å to the pyramidal vertex, whereas the pyramidal base contains two symmetric bonds to S3, 2.623 Å long, and two 3.011 Å distances to S1. The U_{ij} adps of Sb1 are not excessively augmented.

The (Sb,Tl)2 position has the U_{11} coefficient somewhat augmented, a short bond of 2.654 Å to S4 at the vertex, 2×2.649 Å to S7 and 2×3.122 Å to S1 in the base of the pyramid. The S1 ligand has a strong bond only to Sb3. The S7 ligand displays elongation in the [010] direction, i.e., the rod-direction, probably reflecting the substitution by two different cations taking place in the polyhedron center.

Tab. 7 Calculated powder X-ray diffraction data for pokhodyashinite (only reflections with $I_{\text{rel.}} > 1\%$ are listed)

$I_{\text{rel. calc.}} (\%)$	$d_{\text{calc.}} (\text{Å})$	h	k	l
5	10.399	-2	0	1
13	7.298	2	0	1
6	5.841	-4	0	1
6	5.496	4	0	0
3	5.200	-4	0	2
7	4.953	2	0	2
4	4.682	-2	0	3
11	4.547	4	0	1
15	4.401	0	0	3
16	4.220	-4	0	3
21	3.895	-6	0	1
66	3.834	-1	-1	1
13	3.812	-6	0	2
2	3.706	1	-1	1
68	3.671	2	0	3
19	3.508	-3	1	0
36	3.474	-1	-1	2
67	3.466	-6	0	3
10	3.395	-4	0	4
6	3.335	-3	-1	2
24	3.259	3	-1	1
7	3.253	6	0	1
7	3.041	-5	1	1
12	3.028	-6	0	4
100	2.996	-3	-1	3
8	2.971	4	0	3
11	2.969	-5	1	2
32	2.957	-5	1	0
3	2.921	-8	0	2
14	2.905	3	-1	2
6	2.898	-8	0	1
10	2.897	2	0	4
46	2.846	1	-1	3
6	2.817	6	0	2
2	2.808	-8	0	3
5	2.771	-5	1	3
9	2.752	5	-1	1
72	2.748	8	0	0
17	2.631	-3	-1	4
11	2.613	-6	0	5
19	2.609	-1	-1	4
2	2.600	-8	0	4
4	2.556	-7	1	1
3	2.552	-7	1	2
5	2.512	-5	-1	4
25	2.491	5	-1	2
2	2.477	4	0	4
3	2.469	-7	1	0
22	2.457	-7	1	3
34	2.454	6	0	3

The Sb3 position displays an augmented U_{33} component, with displacements along the [001] direction, i.e., to the sides of the rod. Sulfur ligands of this site do not

display excessive displacements in any sense. It has the pyramidal bond of 2.412 Å (to the vertex), 2×2.748 Å to S4 and 2×2.872 Å to S2.

It is the lateral (Sb,Tl)2 position, in which additional, partial substitution of Sb by Tl takes place. This is expressed by the 2.748 Å bond to S4 and a non-fixed character of the S7 ligand.

The *adp* U_{ij} components of the Tl1 site are not excessively large. Distances are 3.160 Å to S3, and 2×3.269 Å which oppose 2×3.298 Å. Opposite to the 3.160 Å bond, there are 2×3.537 Å distances. They manifest the LEP character of Tl⁺ in this structure.

As4 has the $[h0l]$ distance to S5 equal to 2.228 Å (indicating pure As), whereas the diagonally oriented distances, As–S6, are 2.438 Å long. The As–S7 interaction is weak, 2.87 Å, whereas As–S6 (oriented opposite to S5) is 3.31 Å. As4 has a considerably augmented U_{22} component, slightly also the U_{11} component.

Due to its triangular coordination, Cu has large U_{33} , with displacements out of the triangular plane. Horizontal Cu–S3 bond is 2.340 Å, whereas the diagonally oriented bonds to S5 are 2×2.358 Å. The other shorter distance is Cu–S3, equal to 2.717 Å. For comparison, in Cu rich (Cu,Fe) tennantite the tetrahedral $\text{Cu}_{86}\text{Fe}_{14}$ bond is 2.3075 Å, the triangular Cu–S bonds are 2.302–2.310 Å, whereas the planar version of them (ignoring the displacements from the plane of the triangle) is 2.241×2 Å and 2.207 Å (Biagioni et al. 2022). The As–S bond in the AsS₃ pyramid is 2.2655 Å long in this tennantite structure, as opposed by the 2.835 Å long distance to a non-planar triangular Cu site.

Bonding schemes of all cation sites in the pokhodyashinite structure display mirror symmetry on (010), and the short bonds of Sb1 and Sb2 are oriented away from the median plane of the Sb ribbon. For all three Sb sites, these bonds are longer than the expected short Sb–S value. The latter is materialized, however, as the bond to the vertex of the coordination pyramid (see above). The explanation is that the cation is not at the true center of the base of the coordination pyramid, the structure is twinned and the ubiquitous reflection symmetry is a product of twinning. The observed ‘short bonds’ of these coordination polyhedra are combinations (averages) of a true short bond and a medium-long bond, or even of a long non-bonding distance. All this is a result of and testimony to the twinning of a structure, with true symmetry lower than that observed for the twinned structure.

The ‘central’ Sb3 position of the ribbon displays four excessively long Sb–S distances in the pyramidal base; they also show only small differences. This apparently results from averaging two short distances oriented ‘upwards’ with two long distances oriented ‘downwards’ (or oppositely oriented), i.e., not from averaging together the right- and left-hand portions. This agrees with the exact twinning mechanism as above. The hutchinsonite

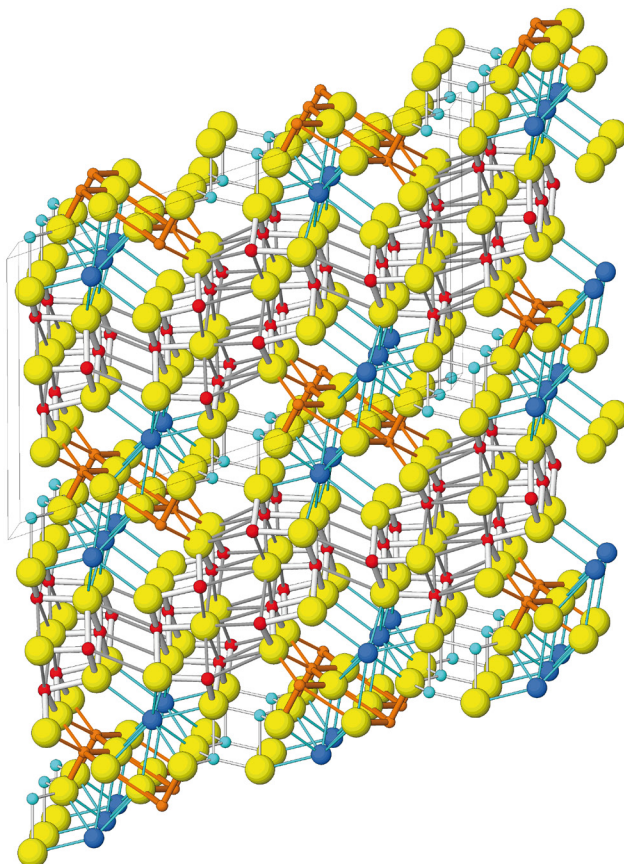
example quoted above lacks such mirror planes and shows schemes of unequal bond lengths in individual polyhedra.

The As4 position indicates practically pure arsenic by the length of its As4–S5 bond, but it illustrates longer remaining bonds distinctly. Again, these represent averages of a short bond and a long As–S distance, it is the latter component that contributes to the resulting excess of the length. The U_{ij} values of As4 confirm this interpretation as well.

With the documented Tl–As–Cu layer configuration (Fig. 5), the hutchinsonite-like arrangement of the described ribbons (i.e., stacking according to the SnS principle) is not possible. Instead of it, they are arranged with alternating orientation, alternatively with two Sb3 sides facing one another and two Sb1 & Sb2 sides oriented against each other (Figs 5a,b). The resulting SnS-like displacements of adjacent double-ribbons are a consequence of this scheme: Interspaces with rod-axis orientation (which is perpendicular to the projection) parallel to [001] of SnS alternate regularly with interspaces which can only be described as rod axes parallel to [010] of SnS. Thus, each double-ribbon has both LEP-based contact orientations, each of them on one surface. This is a rare case among the sulfosalts; the best similar example appears in the crystal structure of lorándite (Fleet 1973; Zemann and Zemann 1979; Balić-Žunić et al. 1995), with similar orientations.

The pairs of double-ribbons which face one another with their Sb1 and Sb2 atoms

a)



b)

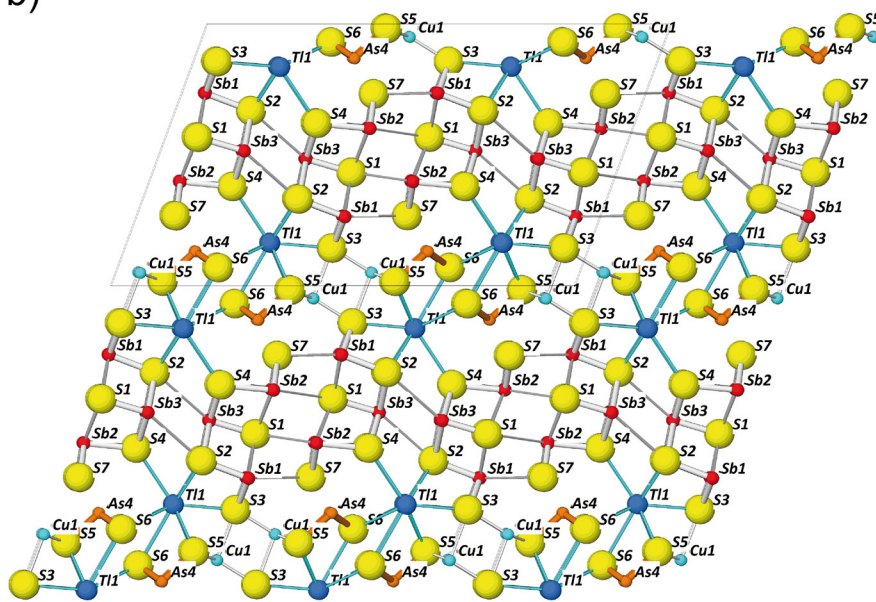


Fig. 5 a – Projection of the crystal structure of pokhodyashinite along [010] (slightly inclined). Tl is shown as blue spheres, Cu/Ag is azure, Sb is orange, As is red, S is yellow. Unit-cell edges are indicated. Weak bonds and LEP contacts are indicated by thin lines. **b** – Labeled atoms and strong bonds versus weak interactions.

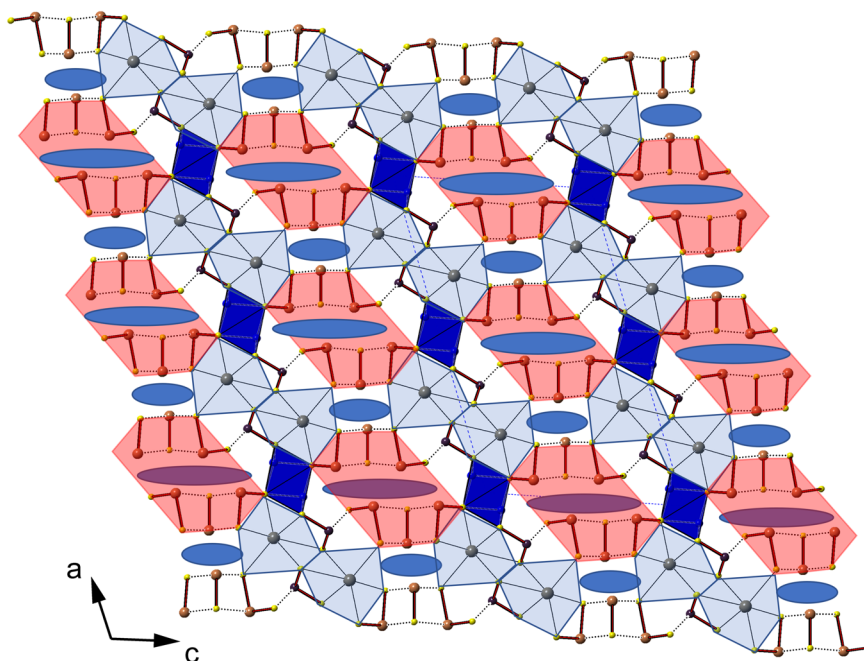


Fig. 6 Arrangement of polyhedral and modular elements in the structure of pokhodyashinite, [010] projection. Coordination polyhedra of Tl are grey, paired trigonal pyramids of Cu are dark blue, four-layer rods of Sb coordinations, with LEP interlayer, are pink and their LEP micelles are indicated by a large ellipse. LEP orientations in the large micelles and small micelles are perpendicular one to another (see Fig. 5a and the text). As: trigonal pyramid close to thallium sites, weak As–S interactions in dashed lines.

(sides) can be interpreted as forming $[010]_{pokho}$ rods with truncated $2H$ and $1Q$ surfaces (Fig. 6) and internal SnS-like match. They are two coordination pyramids broad, isolated and parallel-stacked, forming a resulting thick slab. Unusually, they meet by contacts of two Q surfaces and a contact of a sheared H surface with an H surface. They do not follow the Q -meet- H principle which is common for many Pb–Sb sulfosalts. The Tl coordination polyhedra in the Tl–As–Cu slab can be interpreted as acute tips of these rods, and are surrounded by extra-rod arsenic pyramids as the means of compensation of charge problems. So, pokhodyashinite is a rod structure, but far from being a simple rod-layer structure.

Partially occupied sulfur position S6 is an unusual phenomenon in sulfosalts. It evidently is connected with the partial Tl-for-Sb substitution in the (Sb,Tl)₂ site of pokhodyashinite. This substitution takes place in the original Sb₂ site and leads to the expansion of its coordination polyhedron. Part of this expansion is that the S7 ligands will move away from the Sb₂ site because of longer Tl–S bonds, and they will get closer to the As₄ site, from which they were originally separated by a van der Waals distance. Finally, with increasing substitution, they will bond to S7 instead of S6, and the originally bonded S6 position will be superfluous (i.e., partly vacated), in agreement with the charge balance adjustment connected with the Tl⁺-for-Sb³⁺ substitution. The full occupancy of the S7 site and its somewhat augmented *adps* are in agreement with its role in this substitution process.

7. Conclusions

Pokhodyashinite is a complex sulfosalt of thallium, with two distinct slab-like subunits, one based on ribbon-to-rod-like aggregates of Sb coordination pyramids, the other on combinations of large Tl coordination polyhedra with much smaller As coordination pyramids and paired triangular copper–silver sites. Its overall structural principle can be described as monoclinic, but pronounced twinning of the rare grains available for research does not allow to decide whether the structure is monoclinic or triclinic, only that the [010] reflection plane is missing in the untwinned structure. The partial Tl-for-Sb substitution in the first of the two slab types leads to the flipping of the As position and of the As–S bonds, which results in partial occupancy of one anion site and the formula $(CuAg)TlSb_2Sb_{1-x}Tl_xAs_{7-x}$. The spatial and configurational separation of arsenic and antimony (with partial Tl substitution in the Sb position) is an interesting feature of the pokhodyashinite structure.

Acknowledgments. We thank an anonymous referee and also Yves Moëlo for their friendly criticism and valuable suggestions. Moreover, we thank the anonymous referee for providing us with the structure drawing (Fig. 6), which helped us a lot! The editorial care of Jiří Sejkora is acknowledged as well. We acknowledge CzechNanoLab Research Infrastructure supported by MEYS CR (LM2018110) for financial support for the collection of diffraction data. RŠ thanks the MUNI/A/1570/2021

research project of Masaryk University for support of the WDS study.

Electronic supplementary material. Crystallographic information file for the structure of pokhodyashinite structure is available online at the Journal web site (<http://dx.doi.org/10.3190/jgeosci.342>).

References

- BALIĆ-ŽUNIĆ T, MAKOVICKY E, MOĚLO Y (1995) Contributions to the crystal chemistry of thallium sulphosalts III. The crystal structure of lorándite (TlAsS_2) and its relation to weissbergite (TlSbS_2). *Neu Jb Mineral, Abh* 168: 213–235
- BERLEPSCH P (1996) Crystal structure and crystal chemistry of the homeotypes edenharterite ($\text{TlPbAs}_3\text{S}_6$) and jentschite ($\text{TlPbAs}_2\text{SbS}_6$) from Lengenbach, Binntal (Switzerland). *Schweiz Miner Petrogr Mitt* 76: 147–157
- BERLEPSCH P, MAKOVICKY E, BALIĆ-ŽUNIĆ T (2000) Contribution to the crystal chemistry of Tl-sulfosalts. VI. Modular-level structure relationship between edenharterite $\text{TlPbAs}_3\text{S}_6$ and jentschite $\text{TlPbAs}_2\text{SbS}_6$. *Neu Jb Mineral, Mh* 2000: 315–332
- BIAGIONI C, SEJKORA J, MOĚLO Y, MARCOUX E, MAURO D, DOLNÍČEK Z (2022) Tennantite-(Cu), $\text{Cu}_{12}\text{As}_4\text{S}_{13}$, from Layo, Arequipa Department, Peru: a new addition to the tetrahedrite group minerals. *Mineral Mag*, *in press*, <https://doi.org/10.1180/mgm.2022.26>.
- BOEV T, JOVANOVSKI G, MAKRESKI P (2012) Geology and mineralogy of Allchar Sb–As–Tl–Au deposit. *Geol Maced* 3: 215–233
- BOURGOIN V, FAVREAU G, BOUILLARD J.-C. (2011) Jas Roux (Hautes-Alpes): un gisement exceptionnel à minéraux de thallium. *Le Cahier des Micromonteurs* 113: 2–92 (in French)
- FLEET ME (1973) The crystal structure and bonding of lorándite, $\text{Tl}_2\text{As}_2\text{S}_4$. *Z Kristallogr* 138: 147–160
- KASATKIN AV, MAKOVICKY E, PLÁŠIL J, ŠKODA R, AGAKHANOV AA, KARPENKO VY, NESTOLA F (2018a) Tsygankoite, $\text{Mn}_8\text{Tl}_8\text{Hg}_2(\text{Sb}_{21}\text{Pb}_2\text{Tl})_{\Sigma 24}\text{S}_{48}$, a New Sulfosalt from the Vorontsovskoe Gold Deposit, Northern Urals, Russia. *Minerals* 8: 218
- KASATKIN AV, NESTOLA F, AGAKHANOV AA, ŠKODA R, KARPENKO VY, TSYGANKO MV, PLÁŠIL J (2018b) Vorontsovite, $(\text{Hg}_3\text{Cu})_{\Sigma 6}\text{TlAs}_4\text{S}_{12}$, and Ferrovorontsovite, $(\text{Fe}_3\text{Cu})_{\Sigma 6}\text{TlAs}_4\text{S}_{12}$: The Tl- and Tl–Fe–Analogues of Galkhaite from the Vorontsovskoe Gold Deposit, Northern Urals, Russia. *Minerals* 8: 185
- KASATKIN AV, MAKOVICKY E, PLÁŠIL J, ŠKODA R, CHUKANOV NV, STEPANOV SY, AGAKHANOV AA, NESTOLA F (2019) Gladkovskyite, $\text{MnTlAs}_3\text{S}_6$, a new thallium sulfosalt from the Vorontsovskoe gold deposit, Northern Urals, Russia. *J Geosci* 64: 207–218
- KASATKIN AV, MAKOVICKY E, PLÁŠIL J, ŠKODA R, AGAKHANOV AA, STEPANOV SY, PALAMARCHUK RS (2020a) Luboržákite, $\text{Mn}_2\text{AsSbS}_5$, a new member of pavonite homologous series from Vorontsovskoe gold deposit, Northern Urals, Russia. *Mineral Mag* 84: 738–745
- KASATKIN AV, MAKOVICKY E, PLÁŠIL J, ŠKODA R, AGAKHANOV AA, TSYGANKO MV (2020b) Pokhodyashinite, IMA 2019–130. *CNMNC Newsletter No. 55. Mineral Mag* 84: 485–488
- KASATKIN AV, PLÁŠIL J, MAKOVICKY E, CHUKANOV NV, ŠKODA R, AGAKHANOV AA, STEPANOV SY, PALAMARCHUK RS (2021a) Auerbakhite, $\text{MnTl}_2\text{As}_2\text{S}_5$, a new thallium sulfosalt from the Vorontsovskoe gold deposit, Northern Urals, Russia. *J Geosci* 66: 89–96
- KASATKIN AV, STEPANOV SY, TSYGANKO MV, ŠKODA R, NESTOLA F, PLÁŠIL J, MAKOVICKY E, AGAKHANOV AA, PALAMARCHUK RS (2021b) Mineralogy of the Vorontsovskoe gold deposit (Northern Urals). Part 3: Sulfosalts. *Mineralogiya* 7(2): 5–49 (in Russian).
- KASATKIN AV, PLÁŠIL J, MAKOVICKY E, HORNFECK W, CHUKANOV NV, ŠKODA R, AGAKHANOV AA, TSYGANKO MV (2022a) Gungerite, $\text{TlAs}_3\text{Sb}_4\text{S}_{13}$, a new thallium sulfosalt with a giant structure containing covalent As–As bonds. *Amer Miner*, 107, <https://doi.org/10.2138/am-2022-8003>.
- KASATKIN AV, STEPANOV SYU, TSYGANKO MV, ŠKODA R, NESTOLA F, PLÁŠIL J, MAKOVICKY E, AGAKHANOV AA, PALAMARCHUK RS (2022b) Mineralogy of the Vorontsovskoe gold deposit (Northern Urals). *Mineralogy* 8(1): 5–93.
- KRAUS W, NOLZE G (1996) POWDER CELL – a program for the representation and manipulation of crystal structures and calculation of the resulting X-ray powder patterns. *J Appl Cryst* 29: 301–303
- MAKOVICKY E, (2018) Modular crystal chemistry of thallium sulfosalts. *Minerals* 8: 478
- MAKOVICKY E, PLÁŠIL J, KASATKIN AV, ŠKODA R (2021) The crystal structure of $\text{Tl}_{2.36}\text{Sb}_{5.98}\text{As}_{4.59}\text{S}_{17}$, the lead-free endmember of the chabournéite homeotypic group. *Canad Mineral* 59: 533–549
- MATSUSHITA Y, TAKÉUCHI Y (1994) Refinement of the crystal structure of hutchinsonite, $\text{TlPbAs}_3\text{S}_9$. *Z Kristallogr* 209: 475–478
- MERLET C (1994) An Accurate Computer Correction Program for Quantitative Electron Probe Microanalysis. *Microchim Acta* 114/115: 363–376
- MURZIN VV, BUSHMAKIN AF, SUSTAVOV SG, SHCHERBACHOV DK (1996) Clerite MnSb_2S_4 – a new mineral from Vorontsovskoe gold deposit in the Urals. *Zap Ross Mineral Obsh* 125(3): 95–101 (in Russian)
- MURZIN VV, NAUMOV EA, AZOVSKOVA OB, VARLAMOV DA, ROVNUSHKIN MY, PIRAJNO E (2017) The Vorontsovskoe Au–Hg–As ore deposit (Northern Urals, Russia): Geo-

- logical setting, ore mineralogy, geochemistry, geochronology and genetic model. *Ore Geol Rev* 85: 271–298
- PETŘÍČEK V, DUŠEK M, PALATINUS L (2020) Jana2020. The crystallographic computing system. Institute of Physics, Praha, Czech Republic.
- RABER T, ROTH P (2018) The Lengenbach quarry in Switzerland: Classic locality for rare thallium sulfosalts. *Minerals* 8: 409
- RIGAKU (2019) CrysAlis CCD and CrysAlis RED. Rigaku–Oxford Diffraction Ltd, Yarnton, Oxfordshire, UK
- SAZONOV VN, MURZIN VV, GRIGOR'EV NA (1998) Vorontsovsk Gold Deposit: An Example of Carlin-type Mineralization in the Urals, Russia. *Geol Ore Deposits* 40: 139–151.
- SHELDRICK GM (2015) SHELXT – integrated space-group and crystal-structure determination. *Acta Crystallogr A* 71: 3–8.
- STEPANOV SY, SHARPENOK LN, ANTONOV AV (2017) Fluid-Explosive breccias of the Vorontsovskoe Gold Deposit (The North Urals). *Zap Ross Mineral Obsh* 1: 29–43 (in Russian)
- STEPANOV SY, PALAMARCHUK RS, VARLAMOV DA, KISELEVA DV, SHARPYONOK LN, ŠKODA R, KASATKIN AV (2021) The Features of Native Gold in Ore-bearing Breccias with Realgar-orpiment Cement of the Vorontsovskoe Deposit (Northern Urals, Russia). *Minerals* 11: 541.
- TAKÉUCHI Y, GHOSE S, NOWACKI W (1965) The crystal structure of hutchinsonite, $(\text{Tl, Pb})_2\text{As}_3\text{S}_9$. *Z Kristallogr* 121: 321–348
- VIKENTYEV IV, TYUKOVA EE, MURZIN VV, VIKENTYEVA OV, PAVLOV LG (2016) The Vorontsovsk gold deposit. Geology, gold modes, genesis. *Yekaterinburg, Fort Dialog–Iset*: 1–204 (in Russian)
- ZEMANN A, ZEMANN J (1979) Zur Kenntnis der Kristallstruktur von Lorandit, TlAsS_2 . *Acta Crystallogr* 12: 1002–1006